DRY GRANULAR FLOWS: MICROMECHANICAL INTERPRETATION OF IMPACTS ON RIGID OBSTACLES

Francesco Calvetti, Claudio di Prisco, Irene Redaelli
Politecnico di Milano
francesco.calvetti@polimi.it, claudio.diprisco@polimi.it, irene.redaelli@polimi.it

Emmanouil Vairaktaris
National Technical University of Athens
mvairak@mail.ntua.gr

Abstract

The evaluation of impact forces exerted by flowing granular masses on rigid obstacles is of fundamental importance for the assessment of the associated risk and for the design of protection measures. A number of formulae are available in the literature for the maximum impact force; most of them are based on over-simplifying hypotheses about the behaviour of the granular material. For practical applications, formulations based on either hydrodynamic or elastic body models are often employed. These formulations require the use of empirical correcting factors. In order to better understand the impact mechanics, the authors have recently performed an extensive numerical campaign by using a Discrete Element approach (PFC3D code), where a dry granular mass is represented as a random distribution of rigid spherical particles. A new design formula, combining the hydrodynamic and elastic body theories, has been proposed on the base of the results obtained at the macroscopic scale. The parameters of the formula have been correlated with geometrical factors, namely front inclination and flow height.

In this paper, the same DEM model is further used in order to investigate the relationship between the evolution with time of the impact force and the micromechanics of the granular mass. In particular, information about contact forces and particle velocities will be discussed and critically compared with macroscopic results. In order to progressively introduce the complexity of the impact phenomenon, three geometrical conditions are considered: a) vertical front, confined flow; b) vertical front, free surface flow; c) inclined front, free surface flow.

1. Introduction

The design of shelters for rapid landslide risk mitigation is based on the evaluation of the force exerted on them by the flowing material. Considering the dynamic nature of impacts, the evolution with time of the impact force should be used in design. However, in most practical approaches and standards, a pseudo-static approach is very often considered: the maximum impact force is estimated by using empirical formulae and is quasi-statically applied to the barrier. Very recently, in order to highlight and overcome the limitations of these approaches, the authors have performed a series of simulations using a Discrete Element (DEM) 3D model (Calvetti et al., 2017). A number of factors determining the impact force, namely the geometry of the sliding mass (length, width and flow height, inclination of the front) and the impact velocity, have been considered. The results have been so far interpreted from a macroscopic point of view in terms of maximum impact force, and a new design formula has been introduced accordingly. The maximum average dynamic pressure (Δp_{MAX}) exerted by the granular mass can be written as:
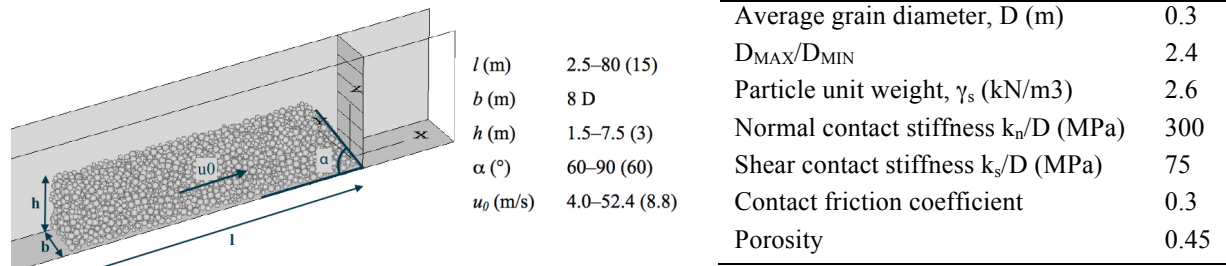
$$\Delta p_{MAX} = a_1 \frac{1}{2} \rho_s u_M u_0 + a_2 \frac{1}{2} \rho_s u_0^2 \qquad (1)$$

where u_0 is the impact velocity, u_M is the propagation velocity of compression waves within the impacting mass and ρ_s is the unit mass of the grains. The first term of Eq. 1 is linear with u_0 and depends on the stiffness and density of the material. This term corresponds to the pressure exerted by the impact of a deformable body on a rigid obstacle. The second term, independent of u_M, is quadratic with u_0 and is analogous to the dynamic pressure exerted by a fluid. The two non dimensional coefficients a_1 and a_2, defining the relative weight of the two components, are a function of material stiffness and front inclination.

Although such finding is very interesting and useful from a practical point of view, the DEM model can provide much more insight into the micro (at the scale of the grains) mechanism determining the global behaviour. For this reason, a new set of simulations have been performed and interpreted from a micromechanical point of view.

2. DEM model

The numerical simulations are performed using the code PFC3D. In the model, the granular mass is assumed to be dry and represented by an assembly of spherical particles whose properties are listed in Fig. 1.

l (m)	2.5–80 (15)
b (m)	8 D
h (m)	1.5–7.5 (3)
α (°)	60–90 (60)
u_0 (m/s)	4.0–52.4 (8.8)

Average grain diameter, D (m)	0.3
D_{MAX}/D_{MIN}	2.4
Particle unit weight, γ_s (kN/m3)	2.6
Normal contact stiffness k_n/D (MPa)	300
Shear contact stiffness k_s/D (MPa)	75
Contact friction coefficient	0.3
Porosity	0.45

Fig 1. 3D view of the DEM model with test conditions (reference values between brackets); model properties

The obstacle is represented by a vertical wall, and plain strain conditions are imposed by confining the flow between two smooth lateral wall elements. The thickness of the channel is equal to 8 D, in order to prevent boundary effects and to limit the numbers of particles in the model. In the case of confined flows, a horizontal wall (not shown in Fig. 1) is added on the top of the model to prevent vertical displacements.

2.1 Simulation procedure and analysis of results

The simulations reproduces the impact process only, while both triggering and propagation phases are disregarded. The impacting granular mass is generated just in front of the obstacle and the impact velocity u_0 is assigned to all particles. Details about the model, simulation procedure and preliminary analyses are presented in Calvetti et al. (2017).

In order to interpret the results, a number of non dimensional variables have been introduced and will be used in the following. f^* is the impact force f normalised by the static force f_s exerted on the obstacle by a fluid with unit weight equal to the unit weight of grains; t^* is time t normalised by the duration t_M of the collision between two average grains:

$$f^* = \frac{f}{f_s}; \quad t^* = \frac{t}{t_M} \tag{2}$$

3. Numerical results

In this section the results of three series of simulations are analysed and the relationship between macroscopic results and the evolution of microscopic data (particle velocity and displacement, contact forces) is illustrated. Reference initial conditions of Fig. 1 are adopted, unless specified.

3.1 Vertical front, confined flow

This condition is the simplest from a mechanical point of view, and reproduces a 1D impact at the macroscopic scale. For this reason, although this case is not realistic, it is very useful for interpreting the underlying mechanics.
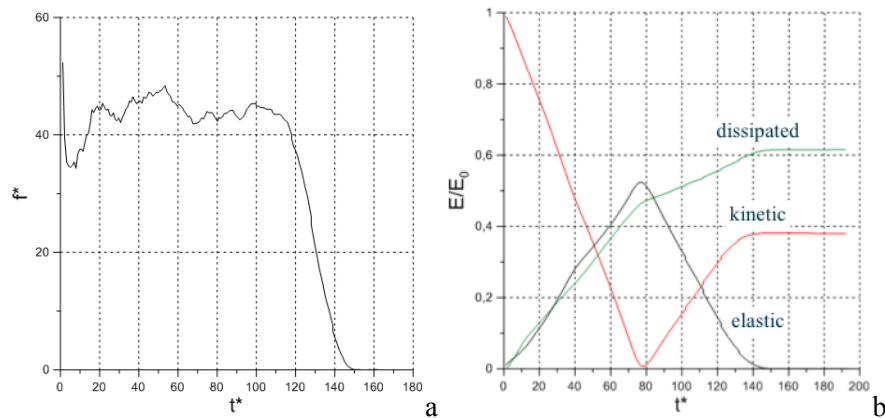
Fig 2. Confined impact, vertical front. Evolution of impact force (a) and energy components (b) with time

The evolution of the impact force (Fig. 2a) is characterised by a sudden peak, followed by a steady condition where it remains almost constant, and a final decrease until it reaches a zero value. In the first phase of the impact ($t^* < 80$), the initial kinetic energy is progressively transformed into elastic energy (i.e., stored in the contacts) and dissipated by contact friction (Fig 2b). Note that the progressive storage of elastic energy takes place essentially under a constant impact force. At approximately $t^* = 80$, kinetic energy has nearly nullified (the velocity of all particles is virtually zero) and has been either stored in contacts or dissipated. For $t^* > 80$, the stored elastic energy is released and transformed back into kinetic energy and dissipated. Note that the rate of energy dissipation is different during the loading and unloading phases.

The mechanics of the described process can be very clearly highlighted by plotting the field of contact forces and particle velocities during the impact (Fig. 3). A quantitative interpretation of the same data is provided in Fig. 4.

The first phase of the impact is characterised by the backward propagation of the compression wave generated when the front particles impact the wall. Note that behind the front of this wave, particle velocities have nullified. In front of it, contact forces are zero.

When the propagation wave reaches the end of the granular mass ($t^* = 80$), all particles have zero velocity and contacts forces are almost uniformly distributed within the mass. From this time instant on, a no-tension wave is reflected from the back of the granular mass towards the obstacle. Behind the front of this wave, particles get a negative velocity (i.e., they bounce back, with a velocity smaller than u_0 because of energy dissipation) and the contact forces network is completely disrupted. All in all, the behaviour of the mass seems to be very similar to that of a deformable elasto-plastic body.

The profiles of average horizontal particle velocities and average horizontal stresses, as a function of the distance to the obstacle are plotted in Fig. 4. Averages are calculated by considering particles and contacts belonging to the same vertical slice, whose width is set to 1 m. Horizontal stresses are calculated from contact forces by using a homogeneisation procedure (Itasca, 2011).

Fig. 4 provides additional information about the transition around the position occupied by the front of the waves. It is worth noting that the width of this zone tends to increase with time, which indicates a progressive increase in disorder within the system. This tendency is particularly evident during the unloading phase.
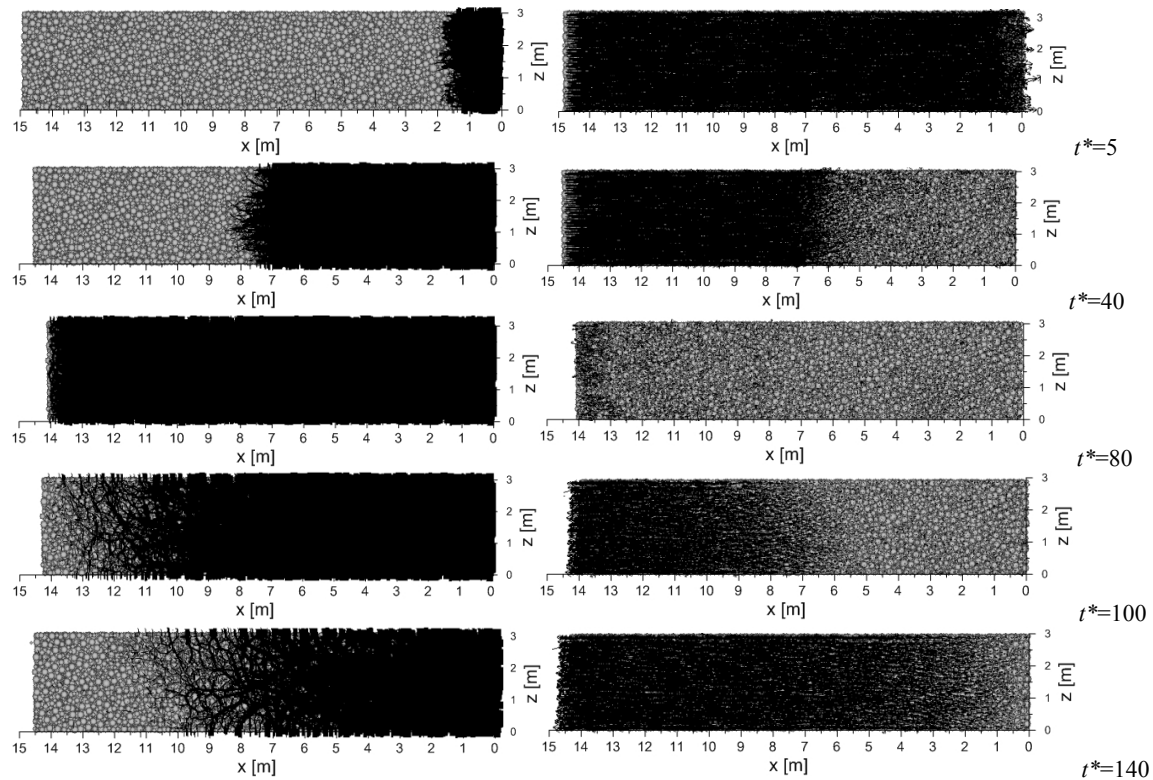
F. Calvetti, C. di Prisco and I. Redaelli

Fig 3. Contact forces (left) and particle velocities (right) at selected time instants. Vertical front, confined flow
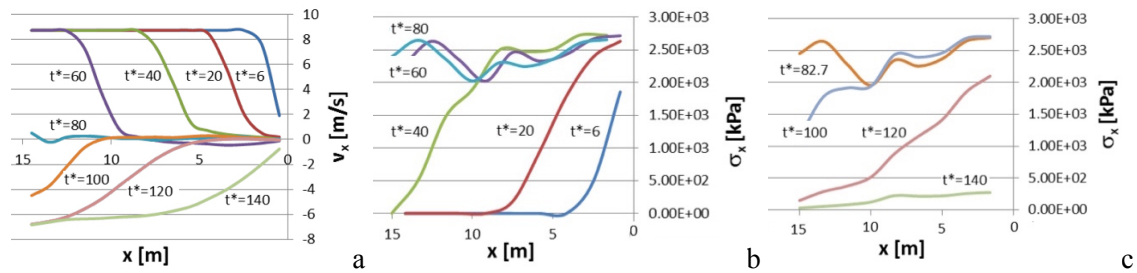

Fig 4. Average horizontal velocity (a) and horizontal stress (b, c) as a function of the distance from the obstacle

3.2 Vertical front, free surface flow

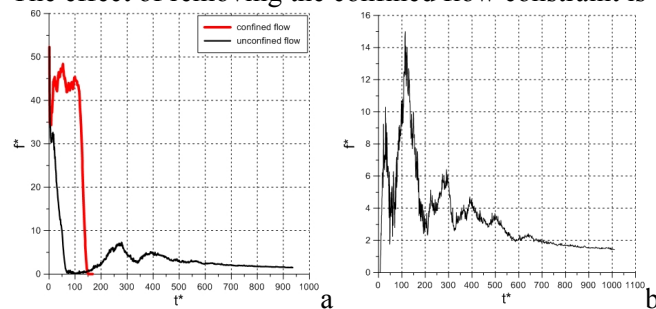The effect of removing the confined flow constraint is evident in Fig. 5a.

Fig 5. Impact force vs. time: (a) confined and free flow, vertical front; (b) inclined front (α=50°)

With the exception of the very first instants, there are both qualitative and quantitative differences between the two conditions: in the unconfined case, the impact force initially decreases very rapidly and is characterised by an irregular trend with two sub-peaks; eventually the impact force decreases to a residual value. The duration of the impact is much longer. In order to understand the reasons of this behaviour it is useful to plot the evolution of the field of contact forces and particle velocities (Fig. 6).

F. Calvetti, C. di Prisco and I. Redaelli
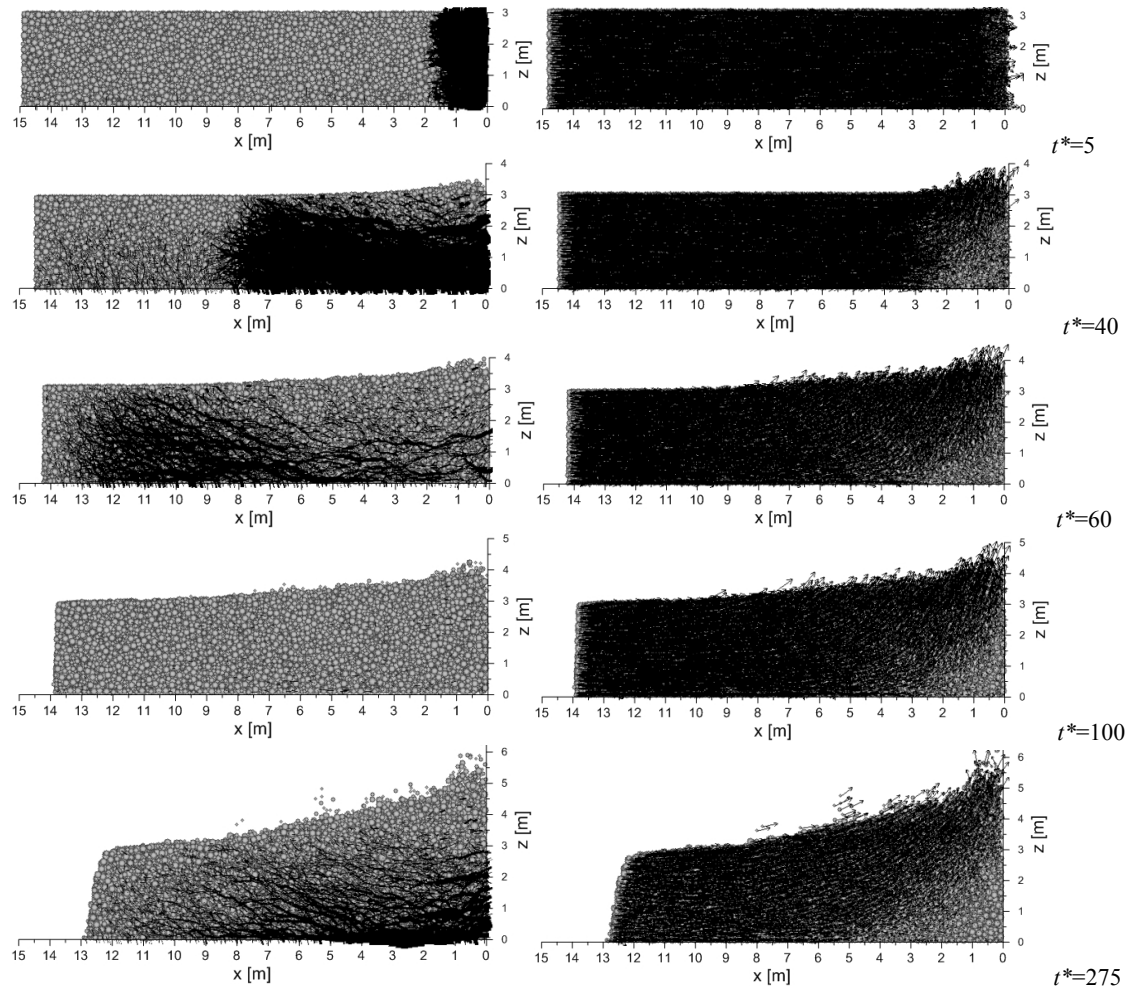
Fig 6. Contact forces (left) and particle velocities (right) at selected time instants. Vertical front, free flow

The initial trend ($t^* < 5$) is identical to that of the confined flow (as it is in terms of impact force). In the following instants, two competing mechanisms are observed: the backward propagation of the compression wave and the buckling of contact force chains. The latter starts from the top of the mass near the obstacle, and propagates downward. A similar effect was observed by Ceccato et al. (2017) who performed analogous simulations using the Material Point Method and attributed the observed behaviour to the formation of vertically directed rarefaction waves. Correspondingly, in the affected region particles are deflected upwards and maintain a horizontal component of velocity; in the same area contact forces tend to zero. At $t^* = 100$, the buckling effect has prevailed (i.e., it has propagated to the bottom of the granular mass): the contact force network has been destroyed and the impact force has nullified. However, a side effect of buckling is that the particles keep a positive horizontal velocity since the equivalent stiffness of the system is strongly reduced. As a consequence, contact forces form again, and the impact force increases again. One or more sub-peaks (two in the case under consideration) may form as a consequence of the observed competing mechanisms. Note in general that the behaviour of the particles is much more disordered in the case of unconfined flow, and that the deformation of the mass is much larger.

3.3 Inclined front, free surface flow

The evolution of impact force with time in the case of inclined front and free surface is shown in Fig. 5b for $\alpha = 50°$. The trend is quite irregular and is characterised by an initial increase until a peak is reached. In the following phases the impact force tends to decrease, although secondary peaks are recorded. The overall duration of the impact is much longer that in the case of vertical front, and the

maximum impact force is much smaller. On the contrary, the residual force is larger. The evolution of the field of contact forces provides clarifying insights for explaining this behaviour (Fig. 7).

t*=40 (first peak)   *t*=55*

t*=120 (second peak)   *t*=200*

t*=300 (third peak)   *t*=900 (residual)*
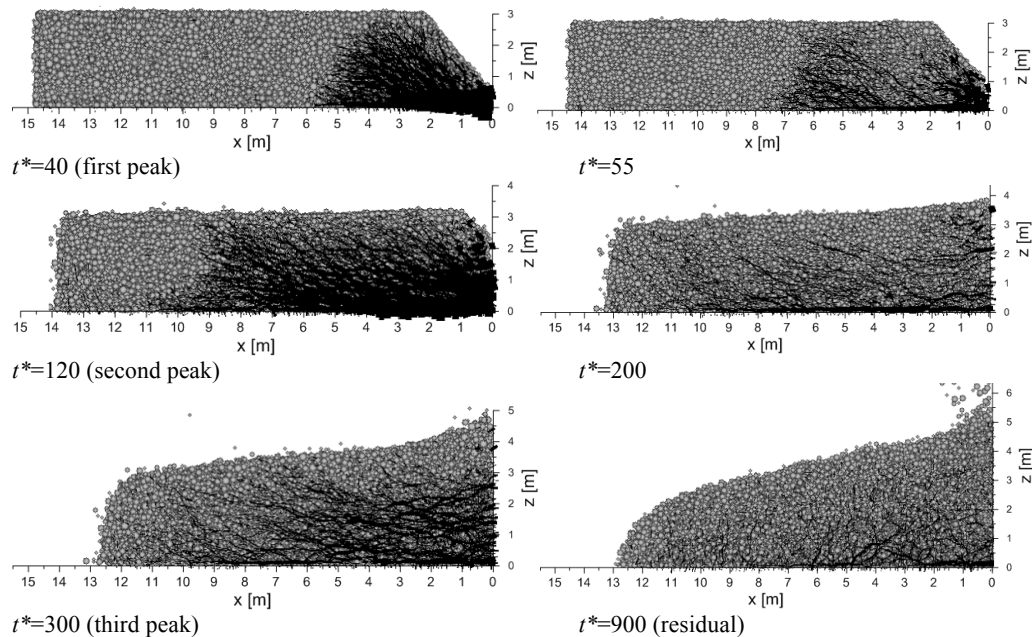
Fig 7. *Contact forces at selected time instants. Inclined front, free flow.*

Besides the features observed in the previous cases (wave propagation, buckling), the inclined front condition is uniquely characterised by a progressive increase in the impact area. Actually, the three mechanisms are competing and determine the irregular trend observed in terms of impact force. It is also evident that in the case of inclined fronts the impact is much more disordered, and the overall behaviour tends to be qualitatively more similar to that of a fluid.

4. Conclusions

In this paper we analysed from a micromechanical point of view the impact of a granular mass on a rigid obstacle. The correlation between macroscopic variables (impact force) and local information (contact forces, particle velocities) allows to understand the mechanisms that are responsible for the complex macroscopic behaviour. In particular, three concurring (in part competing) processes have been highlighted: the propagation of compression and no-tension wave within the mass; the buckling effect; the increase in the contact area between the mass and the obstacle. Depending on the geometry of the impact, these three factors become mutually more or less relevant. In terms of maximum impact force, these considerations justify the need for the formula previously introduced by the authors, where both solid body and hydrodynamic components are included with a relative importance depending on the mentioned factors.

References

Calvetti F., di Prisco C., Vairaktaris E. (2017). "DEM assessment of impact forces of dry granular masses on rigid barriers", *Acta Geotechnica*, 12(1), 129-144.

Calvetti F., di Prisco C., Vairaktaris E. (2016). "Dry granular flows impacts on rigid obstacles: DEM evaluation of a design formula for the impact force". Proc. 6th Italian Conf. of Researchers in Geotechnical Engineering, Bologna, 290-295.

Ceccato F., Simonini P., di Prisco C., Redaelli I. (2017). "The effect of the front inclination on the impact forces transmitted by granular flows to rigid structures". Proc. 4th World Landslide Forum, Ljubljana, 593-600.

Itasca (2011). PFC3D, Theory and background. Itasca, Minneapolis.